RESEARCH ARTICLE OPEN ACCESS

Novel Voltage Regulation Technique for a Three Phase Transformer less Grid Connected Photovoltaic System Using ANN Fractional Order PI Controller

M.Vinay Kumar, U.Salma
Department of Electrical and Electronics Engineering GMR Institute of Technology, RAJAM
Department of Electrical and Electronics Engineering, GIT GITAM University, VISAKAPATNAM
Corresponding author: M.Vinay Kumar

ABSTRACT - In view of protecting the environment, the usage of renewable energy is encouraged from the government agencies since last decade. Amongst the available renewable energy sources (RES), the solar energy source is more advantageous. With increase in concentration of distributed generation (DG) using RES with utility grid, new challenges are introduced and they have to be addressed. One of the challenges is voltage regulation, in this paper AI technique namely ANN along with fractional order PI controller is proposed for voltage regulation of a three phase transformer less grid connected photovoltaic system. Three phase transformer less grid connected photovoltaic system is modelled and simulated in MATLAB/Simulink. The simulation results validates the effectiveness in the performance of the proposed ANN fractional order PI controller as compared with conventional PI controller, fractional order PI controller and fuzzy fractional order PI controller when subjected to various operating conditions like change in solar radiation, change in operating temperature and various loading conditions. The simulation was done with the Neural Network Fitting Toolbox of MATLAB.

Keywords - Solar PV array, MPPT, DC-DC booster, VSI, PI controller, fractional order PI controller, fuzzy fractional order PI controller, ANN fractional order PI controller Matlab/SIMULINK

DATE OF SUBMISSION: 15-01-2020 DATE OF ACCEPTANCE: 31-01-2020

I. INTRODUCTION

Due to rise in population, urbanization and industrialization round the globe, there is a steep hike in demand for electricity. To cope up the demand and protect the environment from pollution alternative environment energy sources have been promoted, these are renewable energy sources (RES) and have lot of advantages over the fossil fuels or conventional energy sources or the non-renewable energy sources (NRES), firstly usage of RES reduces the dependence on fossil fuels, reduces pollution, savings in foreign currency, reduction in huge imports of oils [1-3]. Amongst the RES, solar energy has better edge when compared to other RES due to various reasons like it is abundant in nature, available free of cost. The PV systems uses this solar energy for generation of electricity, when compared with other systems using RES, like less maintenance due to absent of rotating parts, easily expandable as per demand, no production of greenhouse gases like CO_2, So_x, NO_x [4]. The Jawaharlal Nehru National Solar Mission of India was started on the 2010, January 11th, by the Prime Minister with an aspiring target of installing 20,000 MW of solar power connected to grid by 2022 [5]. The limitation of PV system is that it cannot generate electricity through the day due to intermittency in availability of solar energy. International Energy Agency (IEA) predicts that by 2050, globally PV system could generate 11% of electricity and prevent 2.3 giga tonnes of emissions of CO_2 every year [6]. The PV systems can be operated in two modes, Standalone mode and Grid connected mode.

The block diagram of grid connected PV system is shown in figure .1 below

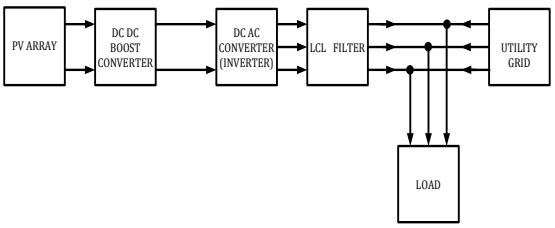

Fig. 1. Block Diagram of Grid Connected PV System

With increase in density of grid connected PV systems to meet the demand for electricity, new challenges and issues get introduced unintentionally. As the power generation of the grid connected PV systems is not continuous due to meteorological conditions, this leads to various issues.

The fractional order (FO) factor can improve the accuracy of controller using FO calculus [7, 8]. The fraction derivatives of the Grunewald–Letnikov (GL) and Riemann–Liouville definition are generally used in FO systems [9, 10]. The conventional PID controller has three controller gainsK_p, K_i, K_d, eliminates steady state error and improves dynamic response, the fractional order PID controller further improves the system performance by tuning of two additional fractional parameters, i.e., integer parameter 'λ' and derivative parameter 'μ'. The fractional order PI controller finds its application in voltage regulation of grid connected solar PV systems [11, 12].The artificial intelligence techniques like FLC,ANN have various applications in field of solar PV systems [13-16]. Fuzzy fractional order PI controller has been used for voltage regulation of grid connected PV system [17,18]. ANN approach has been used for control of the electrical power systems to improve the performance since 1989. The ANN has an ability to be used for non-linear model of complex time-varying system [19]. This is used for voltage regulation of a grid connected PV system. In this paper voltage regulation issue is addressed using artificial neural networks (ANN) fractional order PI controller to enhance the PV system voltage regulation operation.

The rest of the paper is arranged as follows. Section II deliberates modelling of PV system. Section III describes the proposed methodology and simulation results are discussed in Section IV. Conclusion is presented Section V.

.

II. PHOTOVOLTAIC SYSTEM

The photovoltaic system consists of a PV array, a DC-DC boost converter, a VSI and the utility grid.

A. Mathematical model of a Photovoltaic Cell

The basic element of a PV system is PV cell [20, 21], the equivalent circuit of a practical PV cell is shown in figure.2 below

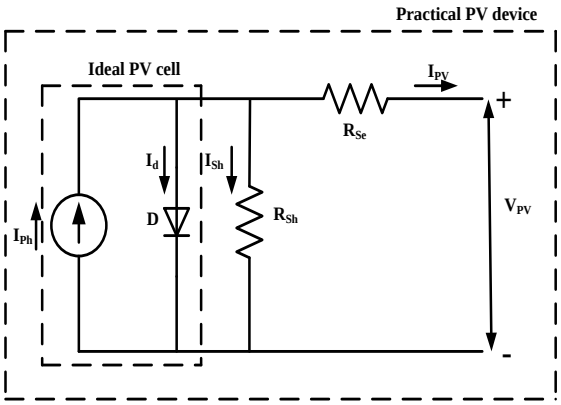

Fig. 2. Ideal and Practical PV Cell

The load current of a PV cell I_{PV} is given as, From KCL

$$I_{PV} = I_{Ph} - I_d - I_{Sh} \quad (1)$$

$$I_{Ph} = [I_{scr} + \lambda(T - T_r)] * \frac{G}{G_r} \quad (2)$$

$$I_d = I_{rs} * \left[e^{\left(\frac{qE_g}{KTA}\right)} - 1\right] \quad (3)$$

$$I_{rs} = I_{rr} * \left(\frac{T}{T_r}\right)^3 * \left[e^{\left(\frac{qE_g}{KTA}\right)*\left(\frac{1}{T_r}-\frac{1}{T}\right)} - 1\right] \quad (4)$$

$$I_{Sh} = \frac{V_{PV} + I_{PV} R_{Se}}{R_{Sh}} \quad (5)$$

The output voltage and current of each PV cell is around 0.5V and 28mA/cm^2 respectively, to obtain higher voltage and currents the cells are connected in series parallel combination. Number of cells connected in series form a PV module, Number of modules connected in series form a PV array, Number of arrays connected in series parallel form a PV panel. The net output current I_{PV} of a PV panel is given as

$$I_{PV} = N_p I_{Ph} - N_p I_{rs} * \left[e^{\left(\frac{qE_g}{KTA\,N_s}\right)} - 1\right] \quad (6)$$

B. Mathematical model of a DC-DC converter

A DC-DC converter converts direct current (DC) voltage from one level to another[22, 23]. The power generated from the solar panel is low and insufficient to supply the load, hence it has to be stepped up using a boost converter, it steps up unregulated DC voltage to a constant output voltageat a higher level. Figure.3 shows the boost converter.

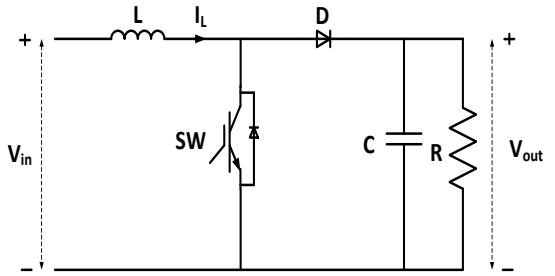

Fig. 3. Boost Converter

It consists of an inductor, a switch a diode and a capacitor. The output voltage is controlled by switch ON and OFF durations and it is called pulse width modulation. The duty cycle k is defined as the ratio of ON duration to the total switching period. Depending upon the switching ON and OFF, energy will be absorbed and released during which the converter operates in continuous conduction mode and dis continuous conduction mode respectively.

$$V_{out} = \frac{1}{V_{in}} k \quad (7)$$

In continuous conduction mode, the switch is in ON mode, the current rises through the inductor and energy is stored in it. The circuit of boost converter in mode-1 is shown in fig.4 below

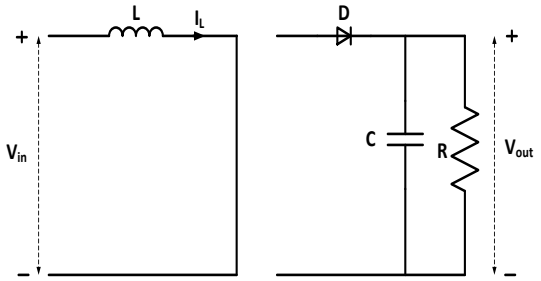

Fig. 4. Boost Converter in Mode-1

For the converter to operate in continuous conduction mode the current through inductor should not fall to zero, the value of inductance is given as

$$L_{min} = \frac{(1-k)^2 kR}{2f}$$

(8)

The output capacitance value is given as

$$C_{min} = \frac{k}{RfV_r}$$

(9)

$$V_r = \frac{\Delta V_{out}}{\Delta V_{out}}$$

(10)

The boost converter waveforms at continuous conduction mode are shown in figure. 5 below

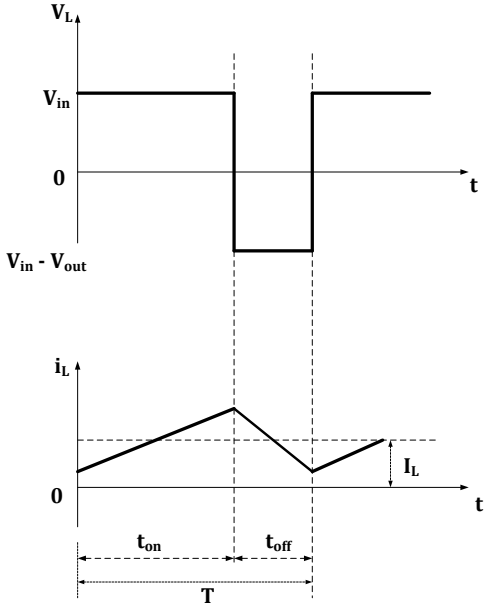

Fig. 5 Boost Converter in Continuous ConductionMode

In discontinuous conduction mode, the switch is in OFF mode, the current flows through the inductor, diode capacitor and the load. The circuit of boost converter in mode-2 is shown in fig.6 below

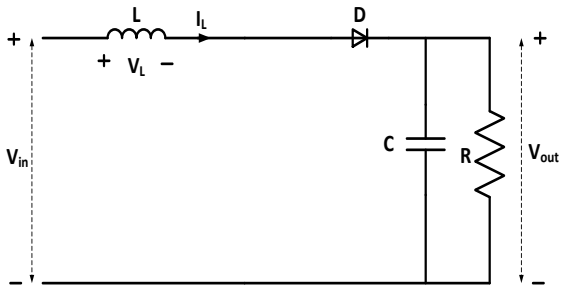

Fig. 6.Boost Converter in Mode-2

The inductor current does not flow continuously, it falls to zero,and integral of inductor voltage over a period of one cycle is zero

$$V_{in}kT + (V_{in} - V_{out})\Delta_1 T = 0$$

(11)

$$V_{out} = \frac{\Delta_1 + k}{\Delta_1} V_{in}$$

(12)

$\Delta_1$is the time duration for negative inductor voltage

The boost converter waveforms for discontinuous conduction mode are shown in figure. 7 below

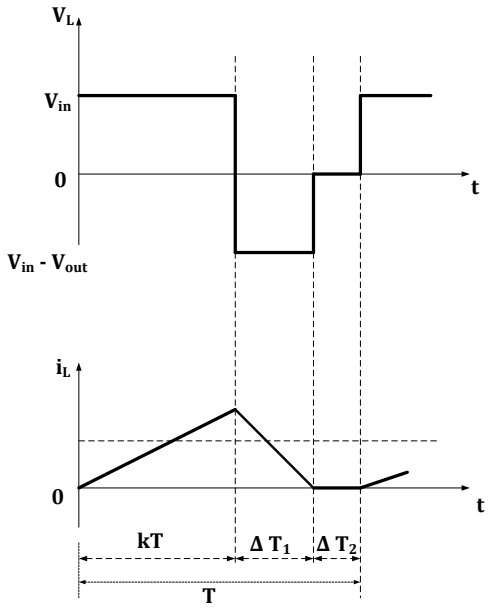

Fig. 7. Boost Converter in Discontinuous Conduction Mode

C. Mathematical model of a PhotovoltaicInverter

The inverter converts the input DC voltage to output AC voltage, a three phase inverter has six arms, each arm has two switches and no two switches of the same arm should be switched ON as it would lead to dead short circuit [24, 25]. The inverter controls both active power and reactive power flow.The circuit of a grid connected three-phase PV inverter is given figure .8 below

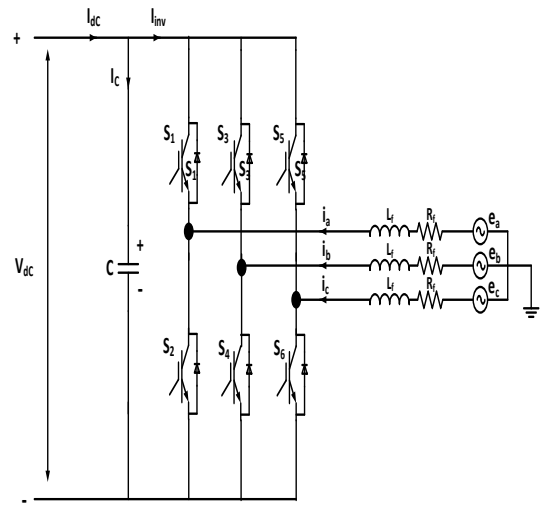

Fig. 8. Grid Connected Three-Phase PV Inverter

The modelling of a grid connected three-phase PV inverter is given below [26]. In a VSI, each arm has two switches and requires a control signal for its operation; no two switches in a single arm (S1 and S2) should be switched ON simultaneously, as complete system will be short circuited in that case. The switching pulses are given by controllers. The grid side filter is represented by R_f and L_f.

The state-space model of VSI in the abc frame as follows

$$\mathrm{i_a} = -\frac{\mathrm{R}}{\mathrm{L}}\mathrm{i_a} - \frac{1}{\mathrm{L}}\mathrm{e_a} + \frac{\mathrm{V_{dc}}}{3\mathrm{L}}(2\mathrm{S_1} - \mathrm{S_2} - \mathrm{S_3}) + \Delta\mathrm{f_1} \quad (13)$$

$$\mathrm{i_b} = -\frac{\mathrm{R}}{\mathrm{L}}\mathrm{i_b} - \frac{1}{\mathrm{L}}\mathrm{e_b} + \frac{\mathrm{V_{dc}}}{3\mathrm{L}}(-\mathrm{S_1} + 2\mathrm{S_2} - \mathrm{S_3}) + \Delta\mathrm{f_2} \quad (14)$$

$$\mathrm{i_c} = -\frac{\mathrm{R}}{\mathrm{L}}\mathrm{i_c} - \frac{1}{\mathrm{L}}\mathrm{e_c} + \frac{\mathrm{V_{dc}}}{3\mathrm{L}}(-\mathrm{S_1} - \mathrm{S_2} + 2\mathrm{S_3}) + \Delta\mathrm{f_3} \quad (15)$$

$$\mathrm{V_{dc}} = \frac{1}{\mathrm{C}}\mathrm{I_{dc}} - \frac{1}{\mathrm{C}}(\mathrm{i_a S_1} - \mathrm{i_b S_2} - \mathrm{i_c S_3}) + \Delta\mathrm{f_4} \quad (16)$$

Where

$$\mathrm{S_i} = \begin{cases} 1 \rightarrow \mathrm{S_i H}\text{: ON}, \mathrm{S_i L}\text{: OFF} \\ 0 \rightarrow \mathrm{S_i H}\text{: OFF}, \mathrm{S_i L}\text{: ON} \end{cases} \quad (17)$$

The transformation matrix is given as

$$\mathrm{T_{dq0}^{abc}} = \frac{2}{3}\begin{bmatrix} \cos(\theta) & \cos(\theta - 120) & \cos(\theta + 120) \\ \sin(\theta) & \sin(\theta - 120) & \sin(\theta + 120) \\ 0.5 & 0.5 & 0.5 \end{bmatrix} \quad (18)$$

The dynamic model (25) in dq model is obtained from [7-10] and is

$$\begin{bmatrix} \mathrm{i_d} \\ \mathrm{i_q} \\ \mathrm{V_{dc}} \end{bmatrix} = \begin{bmatrix} -\frac{\mathrm{R}}{\mathrm{L}} & \omega & \frac{\mathrm{S_d}}{\mathrm{L}} \\ \omega & -\frac{\mathrm{R}}{\mathrm{L}} & \frac{\mathrm{S_q}}{\mathrm{L}} \\ -\frac{\mathrm{S_d}}{\mathrm{C}} & -\frac{\mathrm{S_q}}{\mathrm{C}} & 0 \end{bmatrix}\begin{bmatrix} \mathrm{i_d} \\ \mathrm{i_q} \\ \mathrm{V_{dc}} \end{bmatrix} + \begin{bmatrix} -\frac{1}{\mathrm{L}} & 0 & 0 \\ 0 & -\frac{1}{\mathrm{L}} & 0 \\ 0 & 0 & \frac{1}{C} \end{bmatrix}\begin{bmatrix} i_d \\ i_q \\ V_{dc} \end{bmatrix} + \begin{bmatrix} \Delta f_d \\ \Delta f_q \\ \Delta f_4 \end{bmatrix} \quad (19)$$

Where

$$i_{dq} = T_{dq0}^{abc} . i_{abc} . e_{dq} = T_{dq0}^{abc} . e_{abc} \quad (20)$$

$$\Delta f_{dq} = T_{dq0}^{abc} . \Delta f_{abc}, e_{dq} = T_{dq0}^{abc} . s_{abc} \quad (21)$$

The above mentioned equations can be transformed into two phase stationary frame by Clarke's Transformation

$$T_{\alpha\beta}^{abc} = \frac{2}{3}\begin{bmatrix} 1 & -1/2 & -1/2 \\ 0 & \sqrt{3}/2 & \sqrt{3}/2 \end{bmatrix} \quad (22)$$

The instantaneous power S delivered to the grid is given as

S = P + jQ

Where

$$P = \frac{3}{2}\left(e_d i_d + e_q i_q\right) \quad (23)$$

$$Q = \frac{3}{2}\left(e_d i_q - e_q i_d\right) \quad (24)$$

Where P is the active power and Q is the reactive power In synchronous dq rotating frame, $e_q = 0$

$$P = \frac{3}{2}(e_d i_d) \quad (25)$$

$$Q = \frac{3}{2}\left(e_d i_q\right) \quad (26)$$

D. Mathematical model of a LCL Filter

The total harmonic distortion of three phases should be around 5% as per IEEE 519 standards. The LCL filter is connected between PV system and the grid to filter out the harmonics when injecting power to the grid [27, 28]. A damping resistor is connected to overcome instability caused during resonance by increasing the inductance value of LCL filter. The circuit of a LCL filter is shown in fig.9 below

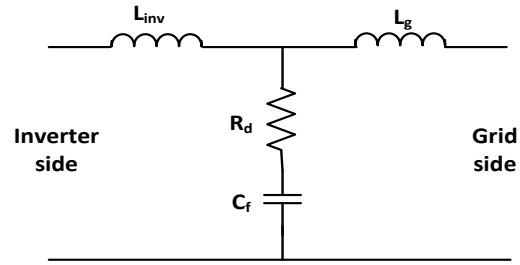

Fig. 9. LCL Filter

The inductance L_{inv} on inverter side is given as

$$L_{inv} = \frac{V_{dc}}{16.\Delta I_{Lmax}.f_s} \quad (27)$$

The rated current at a ripple of 10%, duty cycle of 50% with nominal power and phase voltage is given as

$$\Delta I_{Lmax} = 0.1 * \frac{P_n\sqrt{2}}{3.V_{Ph}} \quad (28)$$

III. PROPSED METHODOLOGY

In this paper AI technique namely ANN along with fractional order PI controller is used for voltage regulation of a three phase transformer less grid connected photovoltaic system.

A. Fractional Order Calculus

Another way of solving nonlinear systems is by using fractional order calculus, in past its application was limited to mathematics, but since few years its application has spread to science and engineering in modelling and control due to its good performance. The fractional order differentiator can be represented by an operator ' ${}_aD_t^\rho$ ' operator for generalization of the differential and integral operators, it is defined as

$${}_aD_t^\rho = \begin{cases} \frac{d^\rho}{dt^\rho} & \rho > 1 \\ 1 & \rho = 1 \\ \int_\rho^t (d\tau)^{-\rho} & \rho < 0 \end{cases} \quad (29)$$

'q' is fractional order and can be a complex number, 'a' is constant relating initial conditions [29-31]. The two commonly used definitions for fractional differentiation and integration are the Grunwald–Letnikov (GL) definition and the Riemann Liouville (RL) definition.The Grunwald–Letnikov (GL) definition is given as

$${}_aD_t^\rho f(t) = \lim_{h\to 0} \frac{1}{h^\rho} \sum_{j=0}^{\frac{t-a}{h}} (-1)^j \frac{\Gamma(\rho-1)}{\Gamma(j+1)\Gamma(\rho-j+1)f(t-jh)} \quad (30)$$

The Riemann Liouville (RL) definition is given as

$${}_aD_t^\rho f(t) = \frac{1}{\Gamma(n-k)} \frac{d^\rho}{dt^\rho} \int_a^t \frac{f(\tau)}{(t-\tau)^{q-\rho+1}} d\tau \quad (31)$$

Where, 'a' is integration limit, step size is 'h', degree of integration/differentiation is 'ρ', gamma function is 'Γ' and is given as

$$\Gamma(t) = \frac{1}{t} \prod_{n=1}^{\infty} \frac{\left(1+\frac{1}{n}\right)^t}{1+\frac{1}{t}} \quad (32)$$

When this fractional calculus is applied to integer controller forms fractional controller

B. Fractional Order PI controller

Fractional order proportional integral derivative (FOPID) controller was proposed by podlunby [23]. The FOPID controller differential equation is given as

$$u(t) = K_p e(t) + K_i D^{-\lambda} e(t) + K_d D^{-\mu} e(t) \quad (33)$$

The proportional constant, the integral constant and the derivative constant are K_p, K_i and K_d. The input and output are $e(t)$ and $u(t)$, the order of the integral and differential is λ and μ

The FOPID controller transfer function is given as

$$C(s) = \frac{U(s)}{E(s)} = K_p + K_i S^{-\lambda} + K_d D^{-\mu} \quad (34)$$

The block diagram for FOPID controller is shown in Fig.10

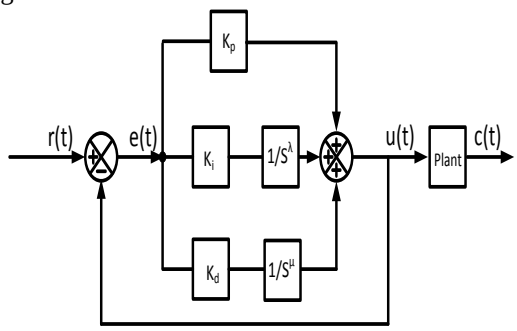

Fig. 10. Block Diagram for FOPID Controller

By tuning the fractional orders λ and μ to one, an integer order PID controller can be obtained and by tuning μ to zero fractional order PI controller is achieved, the FOPI controller transfer function is given as

$$C(s) = \frac{U(s)}{E(s)} = K_p + K_i S^{-\lambda} \quad (35)$$

C. Artificial Neural Network (ANN)

Artificial neural network (ANN) is an intelligence technique which acts similar to human brain, capable of pattern recognition and machine learning. The general schematic of ANN is shown in Fig. 11 below.

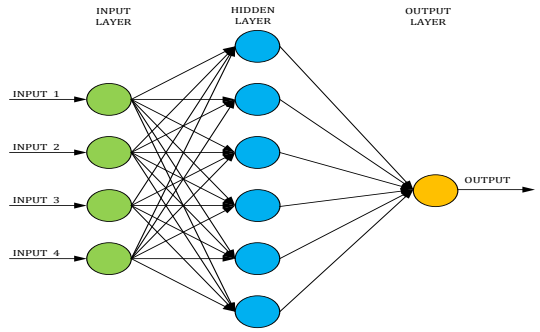

Fig. 11. General Schematic of ANN

It comprises of three layers namely input layer, hidden layer and output layers. The ANN structure is shown in Fig. 12below.

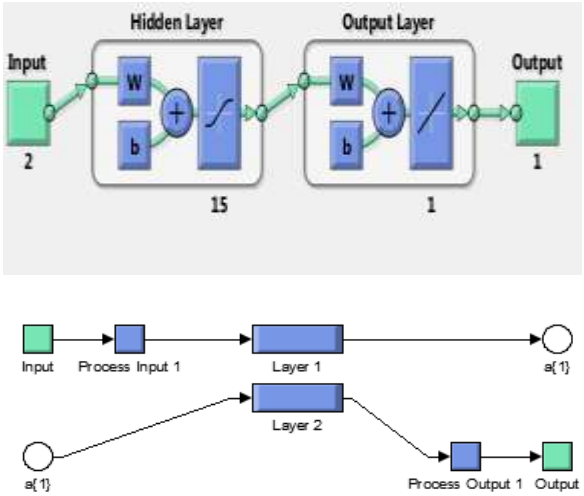

Fig. 12. Neural Network Structure

The structure of ANN with weights and functions is shown in Fig. 13 below.

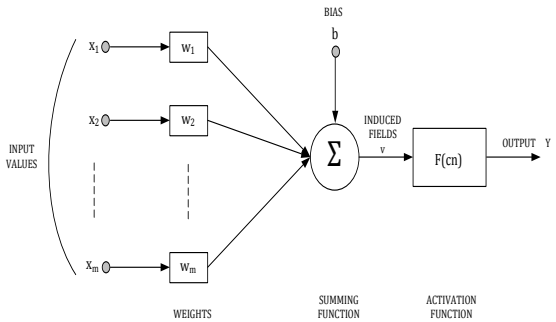

Fig. 13. Structure of ANN with Weights and Functions

The input layer receives data, the output layer sends calculated information and the hidden layers perform the process between the input layer and output layer.All the neurons or part of them in a layer will be connected to all or some neurons of the preceding layer and the next layer through flexible weights as per to the preferred architecture. The set of connection weights has knowledge stored in them.The Neural Network learning is achieved by updating the weights using Feed-Forward back propagation Levenberg-Marquardt algorithm (LMA) with error and change in error as the input of ANN. The LMA is an iterative procedure that finds a local minimum of a multivariable function which is expressed as the squares sum of different non-linear functions. As this matches paramount with the functioning of an ANN, it is carefully chosen to generate the output in ANN by processing the input information.The net is achieved by training (supervised) with trainlm function - Levenberg - Marquardt algorithm, the tolerable for training squared error is 10^{-2}. The neural network performance function is studied using mean square error (MSE) and it is given as

$$E_{MSE} = \sum_{k=1}^{n} \frac{1}{2}[m(k) - d(k)]^2 \quad (36)$$

where the measured output is denoted by m(k) and the desired output is denoted by d(k) denotes and the number of training patterns are denoted by n. The hidden layer has five neurons and tangent sigmoid activation function is used to generate hidden layer output. The linear activation function is used to train the output layer neurons and produce output layer

D. Proposed controller

In this paper, artificial neural network (ANN) FOPI controller is used to enhance the PV system voltage regulation operation. The proposed controller consists of ANN and FOPI controller, as compared to FOPI the proposed controller is robust and stable against variation in parameters, the modified gain values of ANN FOPI controllers are$k_p$and $k_i$are given as

$$k_p = K_p + \Delta K_p \quad (37)$$

$$k_i = K_i + \Delta K_i \quad (38)$$

where K_p, K_i are the proportional gain and integral gain of the FOPI controller and ΔK_p,ΔK_i are the proportional gain and integral gain of the ANN. The block diagram of proposed controller is shown in fig.14 below.

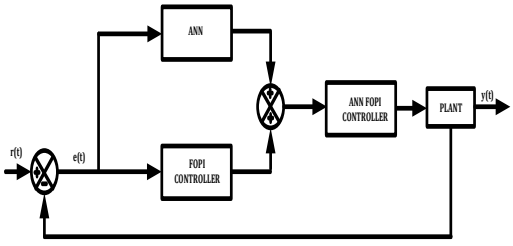

Fig. 14. Block Diagram of Proposed Controller

IV. SIMULATION RESULTS

The three phase grid connected PV system is simulated for checking voltage regulation with different types of controllers like, conventional PI controller, FOPI controller, FFOPI controller and ANNFOPI controller. The simulation results like, DC link voltage, voltage at point of common coupling, active power flow from PV panels to the grid and reactive power flow from PV panels to the grid are presented for different loads like resistive, capacitive and inductive loading are presented.

i. Initial conditions

The DC linc voltage for a solar irradiation of 500 W/m^2 and operating temperature of 25^{0}C is shown in the figure.9 below

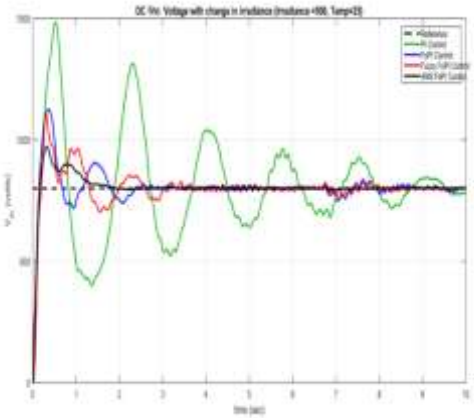

Figure 1.DC Link Voltage

The rise time, settling time, peak overshoot and settling time for the DC linc voltage waveform are less when the system is simulated using ANNFOPI controller as compared to the other controllers like conventional PI controller, FOPI controllerand FFOPI controller.

The voltage at the point of common coupling for a solar irradiation of 500 W/m^2 and operating temperature of 25^{0}C is shown in the figure.10 below

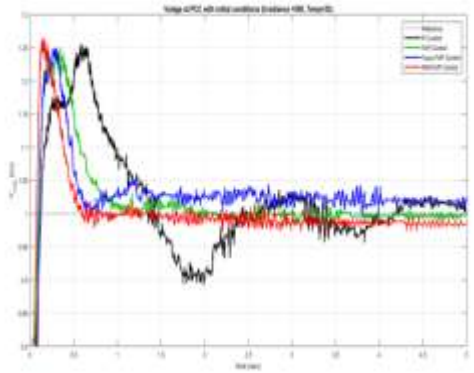

Figure 2. Voltage at the Point of Common Coupling

The rise time, settling time, peak overshoot and settling time for the voltage waveforms at the point of common coupling are less using ANNFOPI controller when compared to the other controllers like conventional PI controller, FOPI controller and FFOPI controller.

The active power flow from PV cell to the grid at initial conditions of solar irradiation of 1000 W/m^2 and operating temperature of 25^{0}C is shown in the figure.11 below

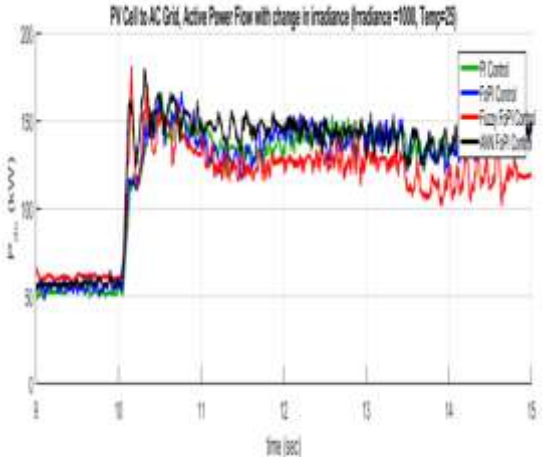

Figure 3. Active Power Flow from PV Panels to the Grid

The rise time, settling time, peak overshoot and settling time for the active power waveforms are less using ANNFOPI controller when compared to the other controllers like conventional PI controller, FOPI controller and FFOPI controller.

The reactive power flow from PV cell to the grid at initial conditions of solar irradiation of 1000 W/m^2 and operating temperature of 25^{0}C is shown in the figure.12 below

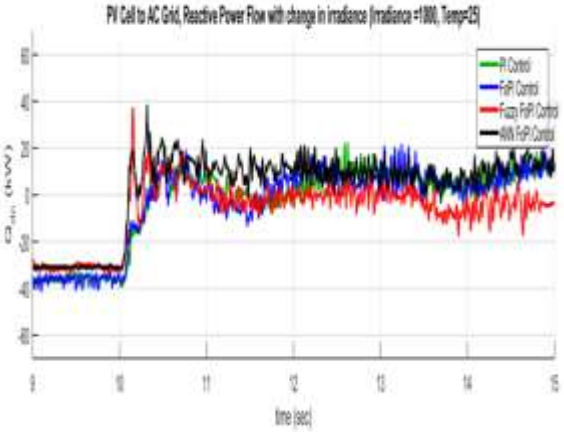

Figure 4. Reactive Power Flow from PV Panels to the Grid

The rise time, settling time, peak overshoot and settling time for the reactive power waveforms

are less using ANNFOPI controller when compared to the other controllers like conventional PI controller, FOPI controller and FFOPI controller.

ii. Capacitive loading

The power at PCC during capacitive load of 500 KVAR for a solar irradiation of 1000 W/m^2 and operating temperature of 25^{0}C is shown in the figure.13 below

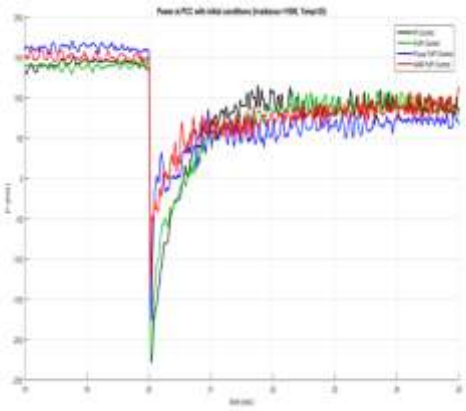

Figure 5. Active Power at PCC During Capacitive Loading

The rise time, settling time, peak overshoot and settling time for active power waveforms at PCC during capacitive load are less using ANNFOPI controller when compared to the other controllers like conventional PI controller, FOPI controller and FFOPI controller.

The reactive power flow from PV cells to the grid during capacitive load of 500 KVAR at solar irradiation of 1000 W/m^2 and operating temperature of 25^{0}C is shown in the figure.14 below

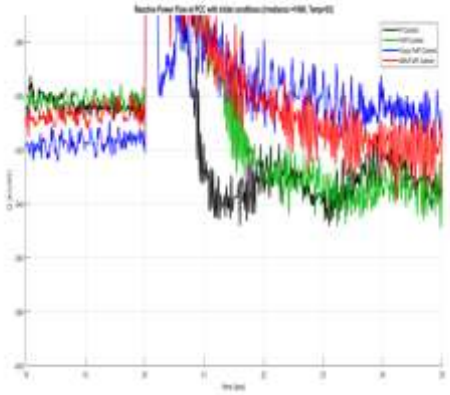

Figure 6. Reactive Power at PCC During Capacitive Loading

The rise time, settling time, peak overshoot and settling time for the reactive power waveforms are less using ANNFOPI controller when compared to the other controllers like conventional PI controller, FOPI controller and FFOPI controller.

The DC linc voltage during capacitive load of 500 KVAR at solar irradiation of 500 W/m^2 and operating temperature of 25^{0}C is shown in the figure.15 below

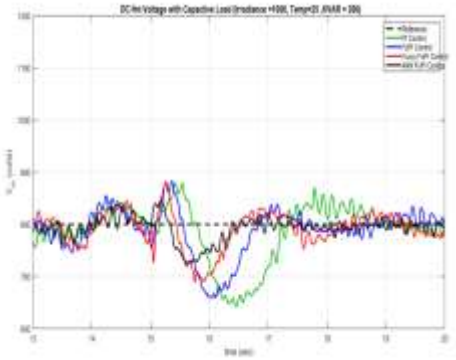

Figure 7. DC Linc Voltage With Capacitive Loading

The rise time, settling time, peak overshoot and settling time for the DC linc voltage waveforms are less using ANNFOPI controller when compared to the other controllers like conventional PI controller, FOPI controller and FFOPI controller.

The voltage at the point of common coupling during capacitive load of 500 KVAR for a solar irradiation of 1000 W/m^2 and operating temperature of 25^{0}C is shown in the figure.16 below

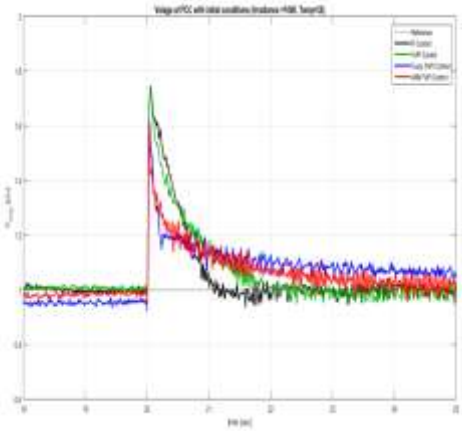

Figure 8. Voltage at Point of Common Coupling With Capacitive Loading

The rise time, settling time, peak overshoot and settling time for the voltage waveform are less using ANNFOPI controller when compared to the other controllers like conventional PI controller, FOPI controller and FFOPI controller.

iii. Inductive loading

The active power flow at PCC during inductive load of 500 KVAR at solar irradiation of

1000 W/m^2 and operating temperature of 25^{0}C is shown in the figure.17 below

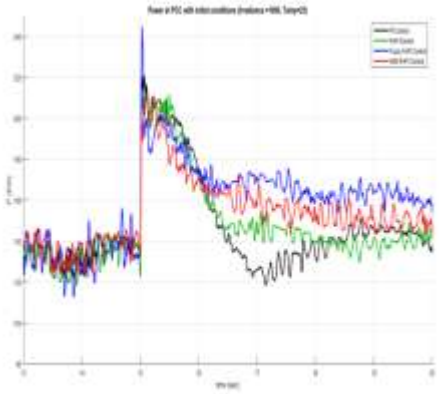

Figure 9. Active Power at PCC With Inductive Loading

The rise time, settling time, peak overshoot and settling time for active power waveforms are less using ANNFOPI controller when compared to the other controllers like conventional PI controller, FOPI controller and FFOPI controller.

The reactive power flow at PCC during inductive load of 500 KVAR at solar irradiation of 1000 W/m^2 and operating temperature of 25^{0}C is shown in the figure.18 below

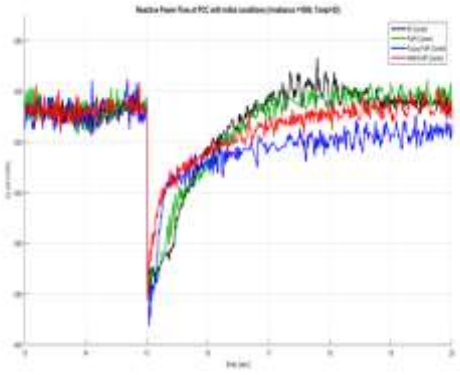

Figure 10. Reactive Power at PCC With Inductive Loading

The rise time, settling time, peak overshoot and settling time for reactive power waveforms are less using ANNFOPI controller when compared to the other controllers like conventional PI controller, FOPI controller and FFOPI controller.

The DC link voltage during inductive load of 500 KVAR at solar irradiation of 1000 W/m^2 and operating temperature of 25^{0}C is shown in the figure.19 below

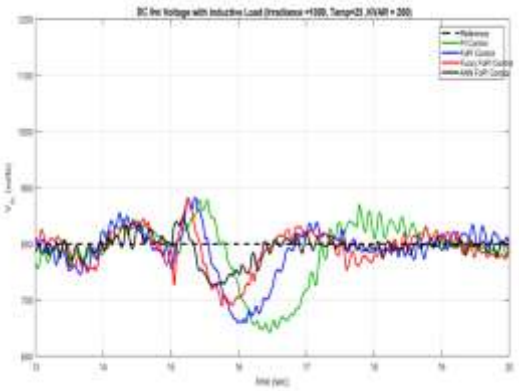

Figure 11. DC Link Voltage With Inductive Loading

The rise time, settling time, peak overshoot and settling time for the DC link voltage waveforms are less using ANNFOPI controller when compared to the other controllers like conventional PI controller, FOPI controller and FFOPI controller.

The voltage at the point of common coupling during capacitive load of 500 KVAR for a solar irradiation of 1000 W/m^2 and operating temperature of 25^{0}C is shown in the figure.20 below

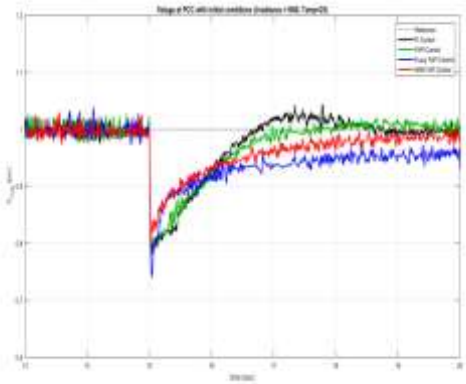

Figure 12. Voltage at the Point of Common Coupling With Inductive Loading

The rise time, settling time, peak overshoot and settling time for the voltage waveforms are less using ANN FOPI controller when compared to the other controllers like conventional PI controller, FOPI controller and FFOPI controller.

V. CONCLUSION

Different controllers namely PI, FOPI, FFOPI and ANNFOPI controllers were used for voltage regulation of a three phase grid connected PV system and was simulated using MATLAB/Simulink software.

The DC link voltage, voltage at point of common coupling, active power flow from PV panels to the grid and reactive power flow from PV

panels to the grid are presented for different loads like resistive, capacitive and inductive loading simulation results are presented and it is concluded that ANNFOPI controller performance was better when compared to the other controllers like conventional PI controller, FOPI controllerand FFOPI controller as the rise time, settling time, peak overshoot and settling time were less using ANNFOPI controller.

REFERENCES

[1]. A. Ashwin Kumar, "A study on renewable energy resources in India", International Conference on Environmental Engineering and Applications, 2010.

[2]. Brendan Banfield, Philip Ciufo, Duane A. Robinson, "The technical and economic benefits of utility sponsored renewable energy integration", Australasian Universities Power Engineering Conference (AUPEC), 2017

[3]. Maher Guizani, Muhammad Anan, "Smart grid opportunities and challenges of integrating renewable sources: A survey", International Wireless Communications and Mobile Computing Conference (IWCMC), 2014

[4]. FisehaMekonnenGuangul, Girma T. Chala, "4th MEC International Conference on Big Data and Smart City (ICBDSC)", 2019

[5]. Jawaharlal Nehru National Solar Mission, Ministry of New and Renewable Energy, Government of India. Available: www.mnre.gov.in/solar-mission/jnnsm/ resolution-2. Accessed: 10th Aug. 2014

[6]. International Energy Agency, Technology Roadmap, Solar Photovoltaic Energy. Available: http://www.iea.org/publications/freepublications/publication/Technology Roadmap Solar Photovoltaic Energy_2014 edition.pdf. Accessed: 15th Aug. 2014

[7]. YangQuan Chen ; Ivo Petras ; DingyuXue, "Fractional order control - A tutorial", American Control Conference, 2009

[8]. DingyuXue, Yangquan Chen, "Fractional Order Calculus and Its Applications in Mechatronic System Controls Organizers", International Conference on Mechatronics and Automation, 2006

[9]. Mithun Chakraborty, DeepyamanMaiti, Amit Konar, RamadossJanarthanan, "A Study of the Grunwald-Letnikov Definition for Minimizing the Effects of Random Noise on Fractional Order Differential Equations", 4th International Conference on Information and Automation for Sustainability, 2008

[10]. Ning Liu, Kui Yao, Yong Shun Liang, "Dimension of Riemann-Liouville fractional integral of Takagi function", Chinese Control And Decision Conference (CCDC), 2018

[11]. K. Sundaravadivu, B. Arun, K. Saravanan, "Design of Fractional Order PID controller for liquid level control of spherical tank", IEEE International Conference on Control System, Computing and Engineering, 2011

[12]. SankalpPaliwal, "Stabilization of Mobile Inverted Pendulum Using Fractional Order PID Controllers", International Conference on Innovations in Control, Communication and Information Systems (ICICCI), 2017

[13]. RecepCakmak, Ismail H. Altas, Adel M. Sharaf, "Modeling of FLC-Incremental based MPPT using DC-DC boost converter for standalone PV system", International Symposium on Innovations in Intelligent Systems and Applications, 2012

[14]. H. Shareef, A. Mohamed, Ammar Hussein Mutlag, "A current control strategy for a grid connected PV system using fuzzy logic controller", IEEE International Conference on Industrial Technology (ICIT), 2014

[15]. Gabriel Mendonça de Paiva, Sergio Pires Pimentel, EnesGonçalvesMarra, Bernardo Pinheiro de Alvarenga, Marco Mussetta, Sonia Leva, "Intra-day forecasting of building-integrated PV systems for power systems operation using ANN ensemble", IEEE conference Milan PowerTech, 2019

[16]. Ragab Ahmed Amer, "ANN Control for a PV-array Connected to Public Grid", Twentieth International Middle East Power Systems Conference (MEPCON), 2018

[17]. Jayanti Singh, Vijander Singh, Asha Rani, Jyoti Yadav, Vijay Mohan, "Performance Analysis of Fractional Order Fuzzy PID Controller for Hybrid Power System Using WOA", 2nd International Conference on Trends in Electronics and Informatics (ICOEI), 2018

[18]. Indranil Pana, Saptarshi Das, "Fractional order fuzzy control of hybrid power system with renewable generation using chaotic PSO", ISA Transactions, Volume 62, pp.19-29, 2016

[19]. Seena Paul, Jaimol Thomas, "Comparison of MPPT using GA optimized ANN employing PI controller for solar PV system with MPPT using incremental conductance", International Conference on Power Signals Control and Computations (EPSCICON), 2014

[20]. A. Durgadevi, S. Arulselvi, S.P. Natarajan, "Photovoltaic modeling and its characteristics", International Conference on Emerging Trends in Electrical and Computer Technology, 2011

[21]. Md. Aminul Islam, Adel Merabet, RachidBeguenane, Hussein Ibrahim, "Modeling solar photovoltaic cell and simulated performance analysis of a 250W PV module", IEEE Electrical Power & Energy Conference, 2013
[22]. VidhyaFulmali, Sujata Gupta, MdFiroz Khan, "Modeling and simulation of boost converter for solar-PV energy system to enhance its output", International Conference on Computer, Communication and Control (IC4), 2015
[23]. Pooja Sahu, Deepak Verma, S Nema, "Physical design and modelling of boost converter for maximum power point tracking in solar PV systems", International Conference on Electrical Power and Energy Systems (ICEPES), 2016
[24]. R. Mechouma, B. Azoui, M. Chaabane, "Three-phase grid connected inverter for photovoltaic systems, a review", First International Conference on Renewable Energies and Vehicular Technology, 2012
[25]. Yu-Jen Liu, Pei-Hsiu Lan, Hong-Hsun Lin, "Grid-connected PV inverter test system for solar photovoltaic power system certification", IEEE PES General Meeting , Conference & Exposition, 2014
[26]. Leonardo P. Sampaio, Moacyr A.G. De Brito , Guilherme De A. E Melo , Carlos A. Canesin, "Grid tie three-phase Inverter with active power injection and reactive power compensation", Renewable Energy, Vol85, pp. 854-864, 2016
[27]. C. Poongothai, Krishna Vasudevan, "Design of LCL filter for grid-interfaced PV system based on cost minimization", IEEE International Conference on Power Electronics, Drives and Energy Systems (PEDES), 2016
[28]. Divya Jain, Ujjwal Kumar Kalla, "Design and analysis of LCL filter for interconnection with grid connected PV system", IEEE 7th Power India International Conference (PIICON), 2016
[29]. R. Caponetto, G. Dongola, L. Fortuna & I. Petras, Fractional Order Systems: Modeling and Control Applications, 2010
[30]. I. Podlubny, "Fractional-order systems and PIλμD controllers," IEEE Trans. on Automatic Control, vol. 44, pp.208–214, 1999
[31]. Podlubny, I., Fractional Differential Equations, Academic Press, Inc., San Diego, CA, USA. 1999
[32]. K. B. Oldham and J. Spanier. The Fractional Calculus: Integrations and Differentiations of Arbitrary Order. New York: Academic Press, 1974

M.Vinay Kumar, et.al. "Novel Voltage Regulation Technique for a Three Phase Transformer less Grid Connected Photovoltaic System Using ANN Fractional Order PI Controller" *International Journal of Engineering Research and Applications (IJERA*), vol.10 (01), 2020, pp 51-61.